Solid State Sciences 20 (2013) 120–126

Contents lists available at SciVerse ScienceDirect

Solid State Sciences

journal homepage: www.elsevier.com/locate/ssscie

Ab initio study of electronic structure, elastic and optical properties of anti-perovskite type alkali metal oxyhalides

J. Ramanna [a], N. Yedukondalu [b], K. Ramesh Babu [b], G. Vaitheeswaran [b,*]

[a] School of Physics, University of Hyderabad, Prof. C. R. Rao Road, Hyderabad 500 046, Andhra Pradesh, India
[b] Advanced Centre of Research in High Energy Materials (ACRHEM), University of Hyderabad, Prof. C. R. Rao Road, Hyderabad 500 046, Andhra Pradesh, India

ARTICLE INFO

Article history:
Received 31 October 2012
Received in revised form
29 January 2013
Accepted 12 March 2013
Available online 26 March 2013

Keywords:
Anti-perovskite
Density functional theory
Band structure
Elastic moduli
Optical properties

ABSTRACT

We report the structural, elastic, electronic, and optical properties of antiperovskite alkali metal oxyhalides Na_3OCl, Na_3OBr, and K_3OBr using two different density functional methods within generalized gradient approximation (GGA). Plane wave pseudo potential (PW-PP) method has been used to calculate the ground state structural and elastic properties while the electronic structure and optical properties are calculated explicitly using full potential-linearized augmented plane wave (FP-LAPW) method. The calculated ground state properties of the investigated compounds agree quite well with the available experimental data. The predicted elastic constants using both PW-PP and FP-LAPW methods are in good accord with each other and show that the materials are mechanically stable. The low values of the elastic moduli indicate that these materials are soft in nature. The bulk properties such as shear moduli, Young's moduli, and Poisson's ratio are derived from the calculated elastic constants. Tran–Blaha modified Becke–Johnson (TB–mBJ) potential improves the band gaps over GGA and Engel-Vosko GGA. The computed TB–mBJ electronic band structure reveals that these materials are direct band gap insulators. The complex dielectric function of the metal oxyhalide compounds have been calculated and the observed prominent peaks are analyzed through the TB–mBJ electronic structures. By using the knowledge of complex dielectric function other important optical properties including absorption, reflectivity, refractive index and loss function have been obtained as a function of energy.

1. Introduction

Anti-perovskite compounds are of much scientific interest because of their versatile physical properties such as giant magneto resistance [1–5], nearly zero temperature coefficient of resistance [6]. Depending on the chemical composition, these materials can display variety of properties such as semiconducting, magnetic and super conducting properties. For example, magnesium based antiperovskites $AsNMg_3$, $SbNMg_3$ exhibit semiconducting properties. Recently the metallic behavior is also found in these materials due to the Mg vacancies [7–9]. Manganese based antiperovskite nitrides ($ANMn_3$, A = Ga, Zn, Cu) interplay a variety of magnetic properties and also exhibit the invar effect and nearly zero temperature coefficient of resistance [6,10]. $NiCMg_3$, $ZnCNi_3$, $CdCNi_3$ are well known superconductors [11–14]. In addition, high Young's modulus of antiperovskite Ti, Sc based anti-perovskite transition metal nitrides Ti_3AlN, Sc_3AlN made them good candidates for aero space applications [15–18].

In view of these important applications of antiperovskites it is worthwhile to know about their physical properties more in detail. Among the known antiperovskite compounds, the alkali metal oxyhalide compounds are relatively unexplored for their physical and chemical properties. Since the structures of these compounds contain unusual combinations of chemical elements it would be quite interesting to know their basic physical and chemical properties. Although these materials possess excellent electronic and bonding properties only few studies are available on these compounds in literature. The crystal structure of Na_3OCl was investigated by Hippler et al. [19] and found to be suitable candidate for determination of the Na^+ Sternheimer antishielding factor due to its cubic crystal symmetry [20,21]. The crystal structure and the related structural properties of K_3OBr were first reported by Sitta et al. [22]. The lattice dynamics and phonon spectrum of the compounds Na_3OCl, Na_3OBr, K_3OBr were studied using force constant method [23]. However, a number of basic properties of these compounds are still unknown. To the best of our knowledge there are no studies from experimental or theoretical side on the

* Corresponding author. Tel.: +91 23138709; fax: +91 40 23010227.
E-mail addresses: gvsp@uohyd.ernet.in, gvaithee@gmail.com (G. Vaitheeswaran).

1293-2558/$ – see front matter © 2013 Elsevier Masson SAS. All rights reserved.
http://dx.doi.org/10.1016/j.solidstatesciences.2013.03.014

electronic, bonding, elastic, and optical properties of these compounds. The knowledge of electronic band structure and density of states is required to understand the conducting nature and the type of bonding present in the materials in terms of the band gap and the hybridization of different atomic states in the materials. They are also useful in understanding the various optical transitions that are possible. The optical properties, such as the absorption spectrum and the dielectric function, can be used to determine the optical band gap and dielectric constants, which are of fundamental importance in modeling the semiconducting devices. The other important physical properties of solids are mechanical properties. The mechanical properties of solids provide important information about the interatomic bonding and the type of forces present in the solids. The elastic constants are indispensable and are useful to know the mechanical behavior and stability of the solids. In this paper, we present a series of first-principles calculations on the structural, electronic, elastic, and optical properties of anti-perovskite alkali metal oxyhalides, Na_3OCl, Na_3OBr, and K_3OBr. The elastic constants and thereby different elastic moduli are calculated which are further used to discuss the mechanical behavior of the metal oxyhalides. The optical properties such as the dielectric function, reflectivity, absorption, refractive index and electron energy-loss function are calculated and discussed. The remainder of the paper is organized as follows. A brief description of methodology is given in Section 2. The results and discussion are presented in Section 3, followed by a brief conclusion in Section 4.

2. Computational details

The first principles calculations were carried out using two different density functional methods, plane wave pseudo-potential (PP-PW) method as implemented in CASTEP code [24,25] and full potential linearized augmented plane wave method (FP-LAPW) as incorporated in WIEN2k package [26]. For plane wave pseudo-potential calculations, we have used ultra-soft pseudo-potentials introduced by Vanderbilt [27] for treating the electron–nuclei interactions. The exchange–correlation (XC) functionals of Ceperley [28] and Alder parameterized by Perdew and Zunger (CA-PZ) [29,30] in local density approximation (LDA) and also the generalized gradient approximation (GGA) of Perdew–Burke–Ernzerhof (PBE) [31] have been used for describing the electron–electron interactions. A plane wave basis set with kinetic energy cut-off of 410 eV for Na_3OCl, Na_3OBr and 420 for K_3OBr has been applied. For the Brillouin zone sampling, the $7 \times 7 \times 7$ Monkhorst–Pack [32] mesh has been used, in which the forces on the atoms are converged to less than 0.01 eV/Å and the total stress tensor is reduced to the order of 0.02 GPa.

In general, the standard DFT functionals LDA, GGA and Engel Vosko (EV)–GGA [33] usually underestimate the energy-band gap about 50% when compared to experiments as they suffer from artificial electron self-interaction and also due to the lack the derivative discontinuities of the exchange–correlation potential with respect to occupation number. In order to get reliable energy band gaps, one has to use more sophisticated methods such as hybrid functionals, GW approximation or TB–mBJ potential [34]. Among them, the later one produces an accurate energy band gaps almost comparable with experiments within a reasonable computation time. Therefore, the electronic structure and optical properties of the investigated compounds were calculated by using this TB–mBJ functional as implemented in WIEN2k package [26]. In order to achieve energy Eigen value convergence, the wave functions in the interstitial region were expanded in plane waves with a cutoff $K_{max} = 8/R_{MT}$, where R_{MT} is the smallest muffin-tin sphere while the charge density was Fourier expanded up to $G_{max} = 14$. The muffin-tin radii were considered to be 2.1, 2.3, 2.0, 2.5 and 2.6 atomic unit (a.u) for Na, K, O, Cl, and Br respectively. Self consistency was obtained using 35 k-points in the irreducible Brillouin zone (IBZ). The frequency dependent optical properties were calculated using dense k-points (286) in IBZ.

3. Results and discussion

3.1. Structural and elastic properties

As a first step, we performed the full structural optimization of the experimental crystal structure of the alkali metal oxyhalides within both LDA as well as GGA using PW-PP and FP-LAPW method within GGA. The calculated ground state properties such as lattice constants using two methods are in good accord with each other and found to be in excellent agreement with the experimental data [19,21,22]. Overall, from the calculated results we observe that the LDA values are underestimated by 2.7% and GGA values overestimated by 1.0%. This might be due to the inherent limitation of density functional theory (DFT) using LDA and GGA functionals. We fitted the total energy–volume data into third-order Birch–Murnaghan equation of state [35] to obtain the bulk modulus values of the compounds. The calculated equilibrium lattice parameters and bulk moduli using two different approaches are given in Table 1.

The elastic constants are fundamental and indispensable for describing the mechanical properties of materials. They also provide information about the mechanical, dynamical behavior and the nature of forces operating in solids, in addition to the mechanical stability and stiffness of materials. The elastic constants of the metal oxyhalides are calculated by applying a set of homogeneous deformations with a finite value and calculating the resultant stress with respect to optimizing the internal atomic coordinates. In general, there are 21 independent elastic constants (C_{ij}) required to describe the asymmetric crystal, but the symmetry of the cubic lattice reduces this number to only three independent elastic constants namely C_{11}, C_{12} and C_{44}. The mechanical stability criteria for a cubic crystal is, its three independent elastic constants should satisfy the following relations given by Born and Huang [36]:

Table 1
Calculated ground state lattice parameter ('a' in Å), bulk modulus (B, in GPa), elastic moduli (C_{ij}, in GPa), shear modulus (G_H, in GPa), Young's modulus (E, in GPa), anisotropy factor (A), Poisson's ratio (σ), and Cauchy's pressure (C_p, in GPa) of alkali oxyhalides Na_3OCl, Na_3OBr and K_3OBr. Experimental data are taken from Refs. [19,21,22].

Parameter	Method	XC	Na_3OCl	Na_3OBr	K_3OBr
a (Å)	PW-PP	LDA	4.381	4.450	4.986
		GGA	4.514	4.609	5.218
	FP-LAPW	GGA	4.543	4.613	5.282
	Expt		4.496	4.573	5.213
B (GPa)	PW-PP	LDA	41.3	39.4	27.1
		GGA	34.2	31.2	20.7
	FP-LAPW	GGA	32.5	31.1	19.9
C_{11} (GPa)	PW-PP	GGA	72.3	62.2	44.6
	FP-LAPW	GGA	68.5	62.1	41.6
C_{12} (GPa)	PW-PP	GGA	15.1	15.7	8.7
	FP-LAPW	GGA	14.4	15.8	7.6
C_{44} (GPa)	PW-PP	GGA	19.7	20.4	11.2
	FP-LAPW	GGA	19.0	19.8	10.6
G_H (GPa)	PW-PP	GGA	22.9	21.5	13.5
	FP-LAPW	GGA	21.9	21.1	12.8
G_H/B	PW-PP	GGA	0.67	0.69	0.65
	FP-LAPW	GGA	0.67	0.67	0.68
E (GPa)	PW-PP	GGA	56.2	52.5	33.3
	FP-LAPW	GGA	53.6	51.6	31.4
A	PW-PP	GGA	0.69	0.87	0.62
	FP-LAPW	GGA	0.70	0.86	0.62
σ	PW-PP	GGA	0.22	0.22	0.23
	FP-LAPW	GGA	0.22	0.22	0.22
C_P (GPa)	PW-PP	GGA	−4.60	−4.76	−2.37
	FP-LAPW	GGA	−4.60	−4.00	−3.00

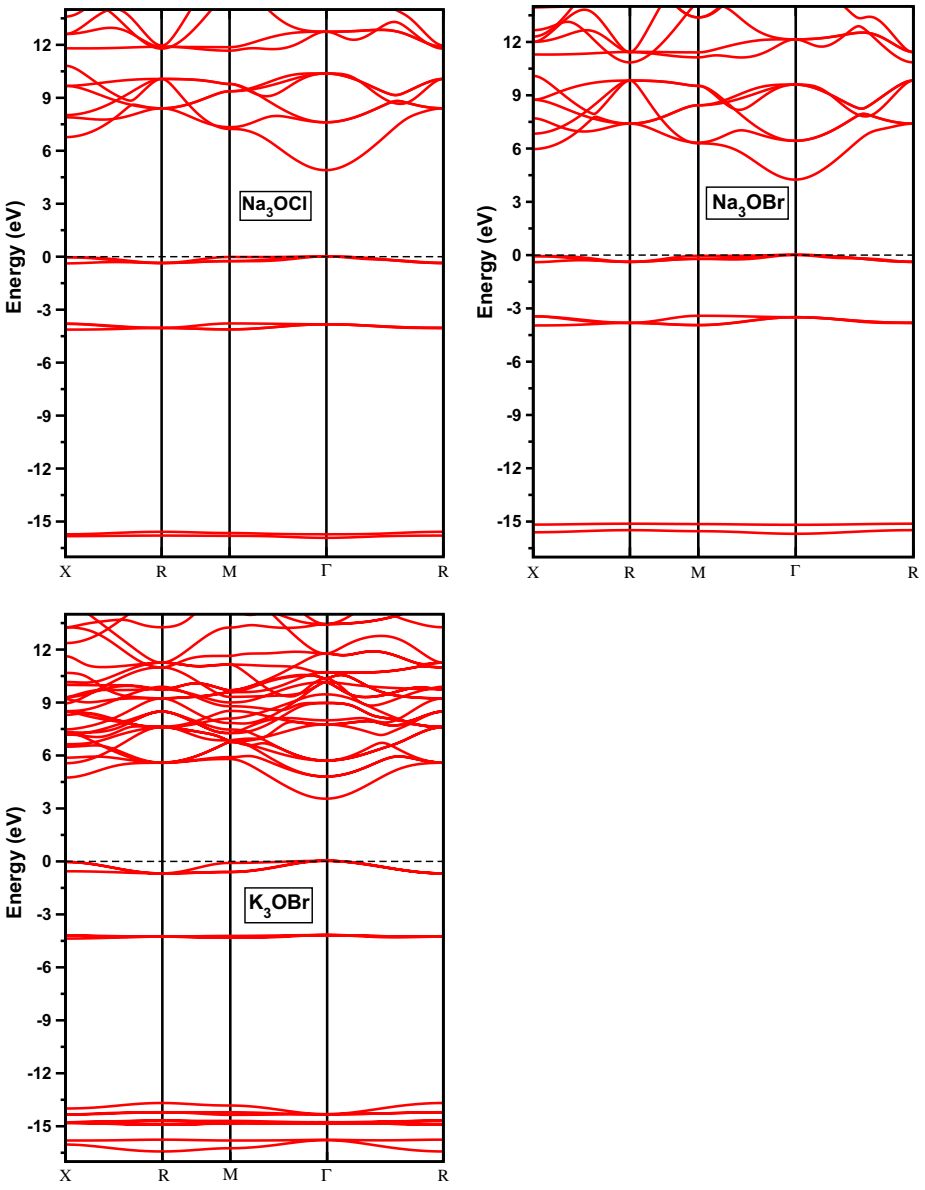

Fig. 1. Electronic band structure of Na_3OCl, Na_3OBr, and K_3OBr calculated using TB–mBJ functional.

$$(C_{11}-C_{12})>0,\ C_{12}>0,\ C_{44}>0, (C_{11}+2C_{12})>0$$

The calculated elastic constants of the three metal oxyhalides follow this stability criteria implying that the three compounds are mechanically stable at ambient pressure. Once the single-crystal elastic constants are computed, the related properties of poly-crystalline aggregates can be evaluated. There are no exact expressions for poly-crystal averaged shear moduli in terms of the C_{ij}, but one can evaluate approximate averages of the lower and upper bounds given Voigt [37] and Reuss [38] approximations. According to Hill [39], the arithmetic average of the Voigt and Reuss values can be used as an estimate to the average shear modulus represented as G_H given by $G_H = (G_R + G_V)/2$. In addition, we also calculate the Young's modulus E, Poisson's ratio σ, which are frequently measured for polycrystalline materials when investigating their hardness.

The ductile–brittle nature of materials is often discussed in terms of elastic constants of the material through the Cauchy's pressure and G/B ratio. The Cauchy's pressure, defined as the difference between the two particular elastic constants C_{12} and C_{44} is considered to serve as an indication of ductility. If the Cauchy's pressure is positive, the material is expected to be ductile while the negative Cauchy's pressure indicates the brittle nature. For the present case, Cauchy's pressure of Na_3OCl, Na_3OBr and K_3OBr is negative, which is a clear indication for the compounds to be brittle in nature. Another index of brittle nature can also be known from the G_H/B ratio, which is also presented in Table 1. According to Pugh's criteria, the high (low) G_H/B ratio is associated with the brittle (ductile) nature of the materials [40]. The critical number which separates the ductile and brittle was found to be 0.57. This ratio is around 0.67 (0.67) for Na_3OCl, 0.69 (0.67) for Na_3OBr and 0.65 (0.68) for K_3OBr, using PW-PP (FP-LAPW) methods, which clearly highlights the brittle nature of the materials. Poisson's ratio generally quantifies the stability of the crystal against shear and takes the value between −1 and 0.5 which are the lower and the upper bounds. The lower bound is where the material does not change its shape and the upper bound is where the volume remains unchanged. The σ value is found to be about 0.22 for Na_3OCl, Na_3OBr, and K_3OBr compounds.

3.2. Electronic structure and optical properties

The electronic band gaps of the alkali metal oxyhalides have been calculated using three different exchange–correlation functionals (GGA–PBE, EV–GGA, TB–mBJ) implemented in WIEN2k package. Among them, the TB–mBJ functional results in improving the energy gaps than rest of the functionals. Koller et al. calculated the electronic band gaps of semiconducting transition metal oxides using TB–mBJ functional which are in very good agreement with experiments [41]. Recently, Dixit et al. calculated electronic band structures of binary and ternary oxides using TB–mBJ potential along with GW calculations. Their study concludes that the calculated band gaps compare well with experiment and GW band gaps [42]. Very recently, Camargo-Martinez et al. calculated electronic band gaps of different type of semi conductors and insulators using TB–mBJ potential which are consistent with experimental results [43]. Hence, we used TB–mBJ functional to calculate the electronic band structures of the alkali metal oxyhalides and are shown in Fig. 1. The calculated TB–mBJ energy gaps are 4.99, 4.35 and 3.65 eV for Na_3OCl, Na_3OBr, and K_3OBr, respectively. The calculated band gap values using three xc functionals are given in Table 2. There are no experimental band gaps available for these compounds to compare with our theoretical band gap values. We hope our calculations will stimulate experiments in this direction. The calculated band structures show that these materials are direct band gap insulators as the band gap occurs along the Γ–Γ direction between the maximum of the valence band and minimum of the conduction band. The electronic density of states (total and partial DOS) gives information about the nature of bonding present in the compounds. The calculated total and partial DOS of the compounds Na_3OCl, Na_3OBr, and K_3OBr are shown in Fig. 2, respectively. The peaks of DOS at the Fermi level are dominated by the *p*-states of oxygen in all the three compounds. The states from halogen atoms are less dominant near the Fermi level and have projections around −5 to −3 eV. In Na_3OCl and Na_3OBr, the *p*-states of halogen and oxygen overlap with *s* and *p*-states of Na atom at the Fermi level. In the valance band region of DOS between −16 and −14 eV, there is an overlap between *p*-states of metal and *s*-states of halogen and oxygen. The overlapping nature becomes stronger from Na_3OCl to Na_3OBr then to K_3OBr, indicating that these are ionic solids with a weak covalent bonding. The conduction band is mainly dominated by *p*-states and less contribution arises from *s*-states of oxygen, halogen and metal atoms (see Fig. 2).

In this section we try to discuss the optical properties of the materials through the knowledge of the calculated electronic band structures. The optical properties of matter can be described by means of the transverse dielectric function $\varepsilon(q,\omega) = \varepsilon_1(\omega) + i\varepsilon_2(\omega)$ where q is the momentum transfer in the photon–electron interaction and ω is the energy transfer. In the present study we have used electric-dipole approximation for the calculations, according to which at $q = 0$, the momentum transfer from the initial state to the final state is neglected. In general there are two contributions to $\varepsilon(\omega)$ namely intraband and interband transitions. The contribution from intraband transitions is important only for the case of metals. The interband transitions can further be split into direct and indirect transitions. The indirect interband transitions involve scattering of phonons. However, the indirect transitions give only a small contribution to $\varepsilon(\omega)$ in comparison to the direct transitions [44], so we have neglected them in our calculations. The direct interband contribution to the absorptive or imaginary part of the dielectric function $\varepsilon(\omega)$ in the random phase approximation [45] without allowance for local field effects is calculated by summing all the possible transitions from the occupied and unoccupied states with fixed k-vector over the Brillouin zone, weighted with the appropriate transition matrix element giving the probability for the transition by

$$\varepsilon_2(\omega) = \frac{Ve^2}{2\pi\hbar m^2\omega^2}\int d^3k \sum |\langle\psi_C|p|\psi_V\rangle|^2 \delta(E_C - E_V - \hbar\omega) \qquad (1)$$

where ψ_C and ψ_V are the wave functions in the conduction and valence bands, p is the momentum operator, ω is the photon frequency, and $\hbar$ is the reduced Planck's constant. The dispersive or real part of the dielectric function $\varepsilon(\omega)$ can be extracted from the Kramers–Kronig relation

$$\varepsilon_1(\omega) = 1 + \frac{2}{\pi}P\int_0^\infty \frac{\varepsilon_2(\omega')\omega' d\omega'}{(\omega')^2 - (\omega)^2} \qquad (2)$$

where '*P*' is the principle value of the integral. In order to calculate $\varepsilon_1(\omega)$ using Kramers–Kronig transformation, it is necessary to evaluate the absorption spectrum to high energies in order to achieve a converged result for the dispersion. So we have calculated $\varepsilon_2(\omega)$ up to 35 eV above the Fermi level. The knowledge of both the real and imaginary parts of the dielectric function allows the calculation of the important optical properties. In this paper, we present and analyze the absorption spectrum $\alpha(\omega)$, reflectivity $R(\omega)$, refractive index $n(\omega)$ and energy-loss spectrum $L(\omega)$ of Na_3OCl, Na_3OBr, and K_3OBr by following the expressions as in Ref. [46].

The prominent peaks in the imaginary part of the dielectric function of Na_3OCl, Na_3OBr and K_3OBr are shown in Fig. 3. In the calculated spectrum of Na_3OCl, peak A at 7.96 eV originates from the transition O 2*p* (at −0.1 eV) → Na 3*s* (at 7.86 eV). The peak B at 9.89 eV arises from the transition O-*p* (at −0.28 eV) → Na 3*s* (at 9.61 eV). The peak C at 12.07 eV is due to the transition from Cl-*p* (at −4.21 eV) → Na 3*s* (at 7.86 eV). The peak D at 13.36 eV probably arises from the transition Cl-*p* (at −4.21 eV) → Na 3*s* (at 9.15 eV). The peak E at 15.94 eV is due to the transition O-*p* (at −4.1 eV) → Cl *s* (at 11.84 eV). In the imaginary part of the dielectric function of Na_3OBr spectrum, the first peak P at 7.02 eV originates from the transition O 2*p* (at −0.11 eV) → Na 3*s* (at 6.91 eV). The peak Q at 10.71 eV arises from the transition Br-*p* (at −3.25 eV) → Na 3*s* (at 7.46 eV). The peak R at 12.21 eV is due to the transition Na-*s* (at −0.11 eV) → O/Br *p* (at 12.10 eV). The peak S at 15.25 eV probably arises from the transition O-*p* (at −3.95 eV) → Br *s* (at 11.3 eV). In the spectrum of K_3OBr, the main peak X at 10.11 eV originates from the transition Br *p* (at −4.22 eV) → K *s* (at 5.89 eV). The peak Y at 13.97 eV arises from the transition Br-*p* (at −4.47 eV) → O *s* (at 9.50 eV). The peak Z at 22.89 eV is due to the transition K-*p* (at −8.77 eV) → O *s* (at 14.12 eV). Overall in all these three compounds, the major optical transitions are mainly from *p* states of O and halogen atoms to the *s* states of metal atoms Na and K, respectively.

The real part $\varepsilon_1(\omega)$ of the dielectric functions for the three alkali oxyhalides Na_3OCl, Na_3OBr, and K_3OBr are also shown in Fig. 3, respectively. The dielectric constant $\varepsilon_1(0)$ of the compounds are given as, 1.97 for Na_3OCl, 2.22 for Na_3OBr, and 2.20 for K_3OBr. The absorption spectrum $\alpha(\omega)$ and photo conductivity of all the three compounds is shown in Fig. 4, respectively. For Na_3OCl and Na_3OBr the absorption starts at 4.88, 4.23 eV whereas for K_3OBr it is from

Table 2
Calculated band gaps (in eV) of alkali oxyhalides Na_3OCl, Na_3OBr and K_3OBr using GGA, EV-GGA and TB–mBJ functionals within LAPW method.

Compound	GGA	EV-GGA	TB–mBJ
Na_3OCl	2.22	2.62	4.99
Na_3OBr	2.06	2.73	4.35
K_3OBr	1.03	1.36	3.65

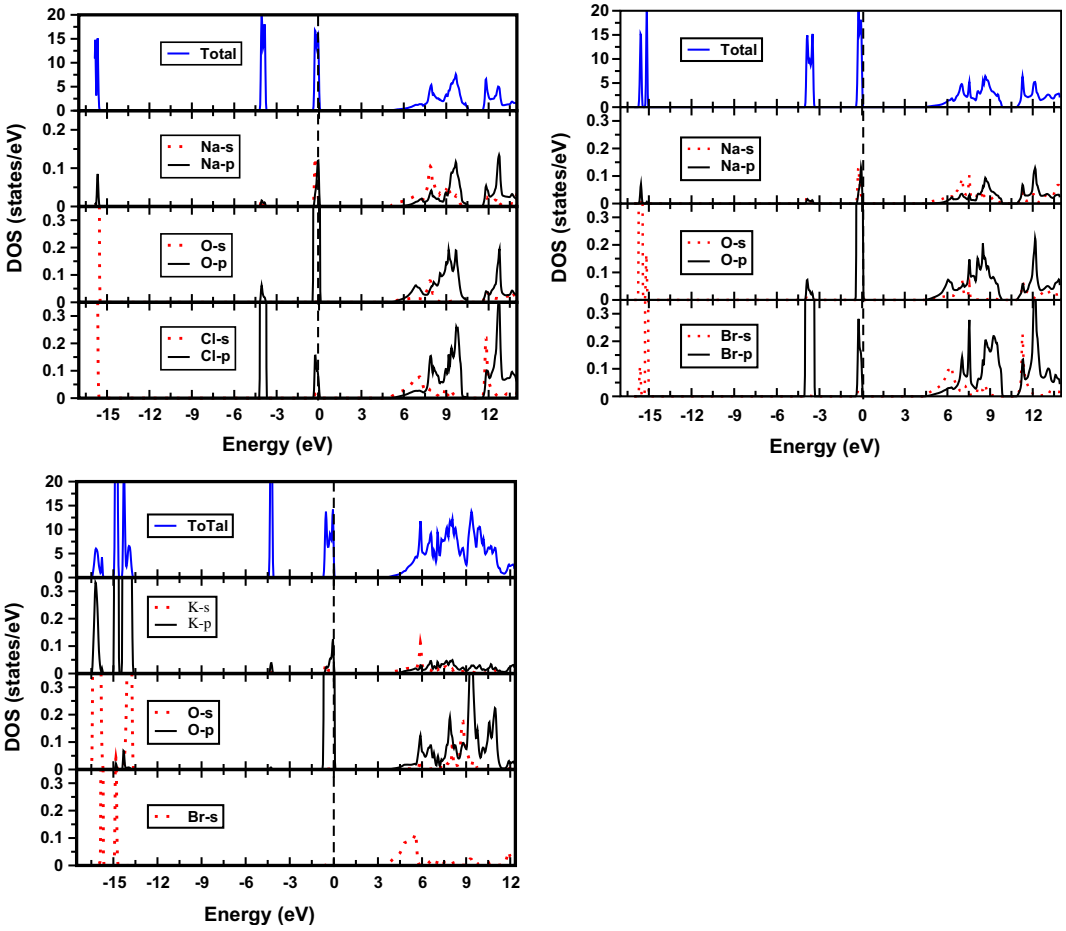

Fig. 2. Total and partial density of states of Na_3OCl, Na_3OBr, and K_3OBr calculated using TB–mBJ functional.

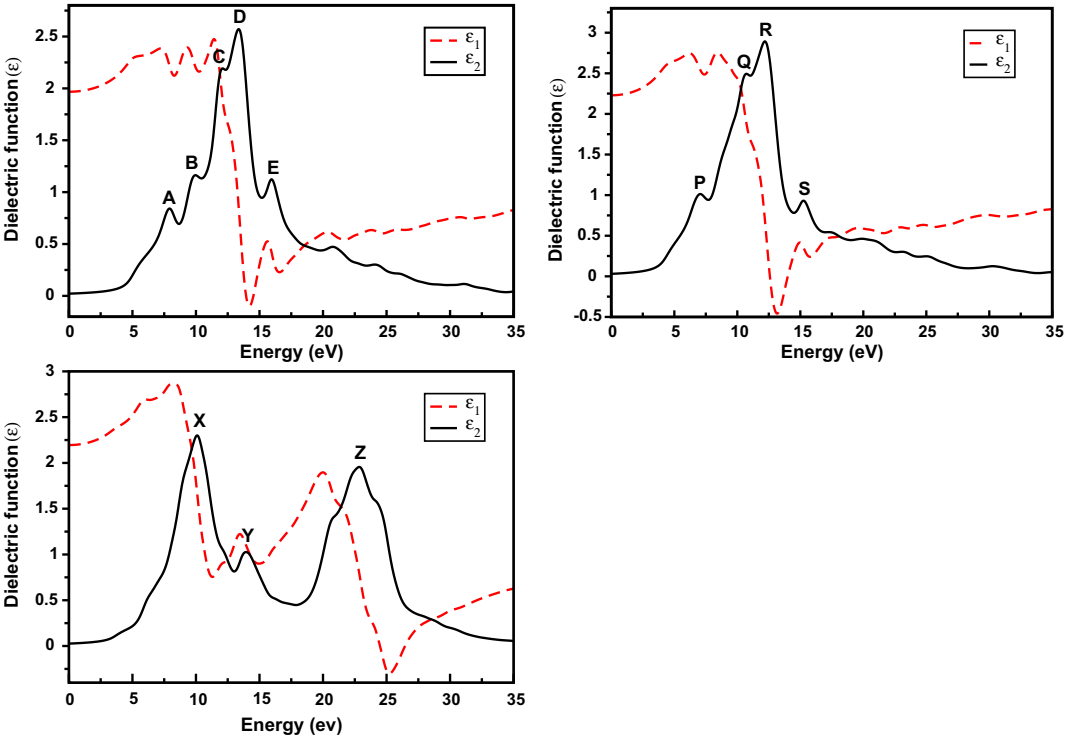

Fig. 3. Complex dielectric function of Na_3OCl, Na_3OBr, and K_3OBr calculated using TB–mBJ functional.

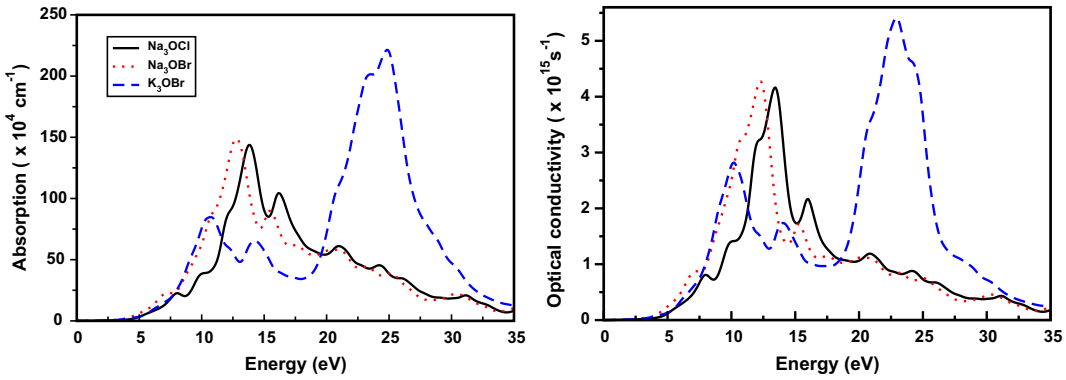

Fig. 4. Absorption and conductivity of Na_3OCl, Na_3OBr, and K_3OBr calculated using TB–mBJ functional.

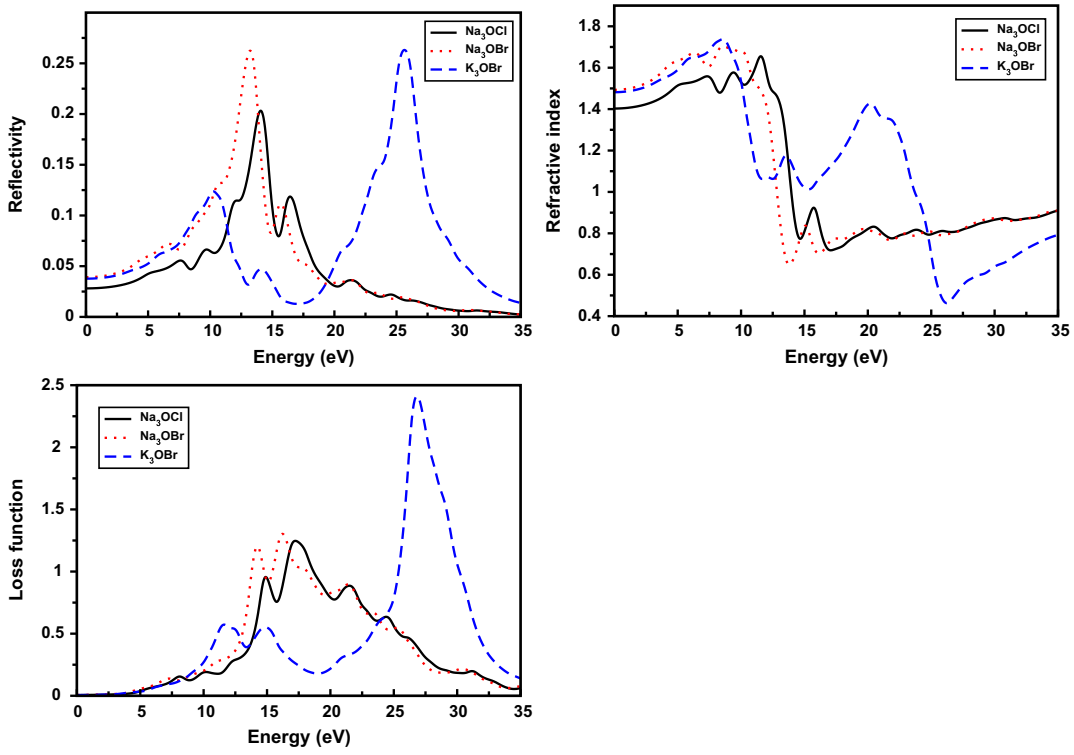

Fig. 5. Reflectivity, refractive index and loss function of Na_3OCl, Na_3OBr, and K_3OBr calculated using TB–mBJ functional.

3.56 eV, these values merely indicate the optical band edge of the materials. The peaks in the absorption spectrum are due to the transitions from valence to conduction bands. Optical conductivity is the increase in the number of free carriers generated when photons are absorbed. From the optical conductivity spectrum, it is found that all the three compounds have broad photocurrent response from 0 to 35 eV. The reflectivity spectrum, complex refractive index and the loss function of all the three compounds are shown in Fig. 5, respectively. The reflectivity spectrum of all the three compounds mainly contains 6 peaks. The maximum reflection occurs at 14.09 eV in Na_3OCl and at 13.24 eV in Na_3OBr whereas for K_3OBr it is observed at 25.63 eV. The calculated refractive index spectrum (real part) clearly shows the $n\,(0)$ values of 1.40, 1.49, and 1.48 for Na_3OCl, Na_3OBr, and K_3OBr, respectively. The electron energy loss function $L\,(\omega)$ is an important optical parameter in describing the energy loss of a fast electron traversing in a certain material. The peaks in the $L\,(\omega)$ spectra represent the characteristics associated with the plasma resonance and the corresponding frequency is so-called plasma frequency above which the material is dielectric $(\varepsilon_1\,(\omega)) > 0$ and below which the material behaves like a metallic compound $(\varepsilon_1\,(\omega)) < 0$. The peaks in the $L\,(\omega)$ spectra are the trailing edges in the reflection spectra. For instance, the peaks in $L\,(\omega)$ at 17.23, 16.20, 26.83 eV correspond to the abrupt reduction of reflectivity in Na_3OCl, Na_3OBr, and K_3OBr respectively.

4. Conclusions

In the present study, we have systematically studied the structural and elastic properties of antiperovskite Na_3OCl, Na_3OBr and K_3OBr using plane wave pseudo-potential method whereas electronic structure and optical properties of these compounds using FP-LAPW method based on density functional theory. The obtained ground state properties are in excellent agreement with the available experiments, especially our calculated values within GGA are close to experiments compared to LDA results. The calculated elastic constants reveal that the studied materials are mechanically stable and are brittle in nature. From the calculated band structure

and density of states, it is concluded that these compounds are direct band gap insulators and also a considerable enhancement is obtained in the band gap of these materials using TB–mBJ functional over EV–GGA and GGA–PBE. The band gap is reduced highly when Na atom is replaced by K, but it is less pronounced when Cl atom is replaced by Br. The imaginary and real part of the dielectric function of three compounds has been calculated. From this the other optical properties such as absorption, photo conductivity, reflectivity, refractive index and loss function are derived. It is found that all the three materials have broad absorption spectrum in the range of 0–35 eV. Our investigations provide a useful information for potential application of these materials.

Acknowledgments

JR wishes to thank HCU for financial support. NYK and KRB would like to thank DRDO through ACRHEM for the financial support. All the authors acknowledge CMSD, University of Hyderabad for providing the computational facility.

References

[1] W.S. Kim, E.O. Chi, J.C. Kim, H.S. Choi, N.H. Hur, Solid State Commun. 119 (2001) 507.
[2] B.S. Wang, P. Tong, Y.P. Sun, X. Luo, X.B. Zhu, G. Li, X.D. Zhu, S.B. Zhang, Z.R. Yang, W.H. Song, J.M. Dai, Europhys. Lett. 85 (2009) 47004.
[3] D.A. Joshi, N. Kumar, A. Thamizhavel, S.K. Dhar, Phys. Rev. B 80 (2009) 224404.
[4] A. Pandey, C. Mazumdar, R. Ranganathan, Appl. Phys. Lett. 94 (2009) 172509.
[5] Y. Wen, C. Wang, Y. Sun, M. Nie, L. Fang, Y. Tian, Solid State Commun. 149 (2009) 1519.
[6] E.O. Chi, W.S. Kim, N.H. Hur, Solid State Commun. 120 (2001) 307.
[7] E.O. Chi, W.S. Kim, N.H. Hur, D. Jung, Solid State Commun. 121 (2002) 309.
[8] C. Loison, A. Leithe-Jasper, H. Rosner, Phys. Rev. B 75 (2007) 205135.
[9] A.S. Mikhaylushkin, C. Höglund, J. Birch, Zs. Czigány, L. Hultman, S.I. Simak, B. Alling, F. Tasnádi, I.A. Abrikosov, Phys. Rev. B 79 (2009) 134107.
[10] K. Takenaka, H. Takagi, Appl. Phys. Lett. 87 (2005) 261902.
[11] T. He, Q. Huang, A.P. Ramirez, Y. Wang, K.A. Regan, N. Rogado, M.A. Hayward, M.K. Haas, J.S. Slusky, K. Inumam, H.W. ZZandbergen, N.P. Ong, R.J. Cava, Nature 54 (2001) 411.
[12] M.S. Park, J.S. Giim, S.H. Park, Y.W. Lee, S.I. Lee, E.J. Choi, Supercond. Sci. Technol. 17 (2004) 274.
[13] M. Uehara, T. Amano, S. Takano, T. kori, T. Yamazaki, Y. Kimishima, Physica C 440 (2006) 6.
[14] G. Vaitheeswaran, V. Kanchana, A. Svane, A. Delin, J. Phys. Condens. Matter 19 (2007) 326214.
[15] M. Magnuson, M. Mattesini, C. Hogulung, I.A. Abrikosov, J. Birch, L. Hultman, Phys. Rev. B 78 (2008) 235102.
[16] J.C. Schuster, J. Bauer, J. Solid State Chem. 53 (1984) 260.
[17] V. Kanchana, Europhys. Lett. 87 (2009) 26006.
[18] V. Kanchana, Swetarekha Ram, Intermetallics 23 (2012) 39–48.
[19] K. Hippler, S. Sitta, P. Vogt, H. Sabrowsky, Acta Crystallogr. C 46 (1990) 736–738.
[20] G. Klösters, M. Jansen, Solid State Nucl. Magn. Reson. 16 (2000) 279–283.
[21] H. Sabrowsky, K. Paszkowski, D. Reddig, P. Vogt, Z. Naturforsch. 43B (1988) 238.
[22] S. Sitta, K. Hippler, P. Vogt, H. Sabrowsky, Z. Anorg. Allg. Chem. 597 (1991) 197–200.
[23] V.I. Zinenko, N.G. Zamkova, Ferroelectrics 265 (2002) 23–29.
[24] M.C. Payne, M.P. Teter, D.C. Allen, T.A. Arias, J.D. Joannopolous, Rev. Mod. Phys. 64 (1992) 1045.
[25] M.D. Segall, P.J.D. Lindon, M.J. Probert, C.J. Pickard, P.J. Hasnip, S.J. Clark, M.C. Payne, J. Phys. Condens. Matter 14 (2002) 2717–2744.
[26] P. Blaha, K. Schwarz, G.K.H. Madsen, D. Kvasnicka, J. Luitz, in: K. Schwarz (Ed.), WIEN2K, An Augmented Plane Wave + Local Orbitals Program for Calculating Crystal Properties, Technical Universitat, Wien, Austria, 2001, ISBN 3-9501031-1-2.
[27] D. Vanderbilt, Phys. Rev. B 41 (1990) 7892.
[28] D.M. Ceperly, B.J. Alder, Phys. Rev. Lett. 45 (1980) 566.
[29] J.P. Perdew, A. Zunger, Phys. Rev. B 23 (1981) 5048.
[30] J.P. Perdew, A. Zunger, Phys. Rev. B 45 (1992) 13244.
[31] J.P. Perdew, K. Burke, M. Ernzerhof, Phys. Rev. Lett. 77 (1996) 3865.
[32] H.J. Monkhorst, J.D. Pack, Phys. Rev. B 13 (1976) 5188.
[33] E. Engel, S.H. Vosko, Phys. Rev. B 47 (1993) 13164.
[34] F. Tran, P. Blaha, Phys. Rev. Lett. 102 (2009) 226401.
[35] F. Birch, Phys. Rev. 71 (1947) 809.
[36] D.C. Wallace, Thermodynamics of Crystals, Wiley, New York, 1972.
[37] W. Voigt, Ann. Phys. (Leipzig) 38 (1889) 573.
[38] A. Reuss, Z. Angew. Math. Phys. 9 (1929) 49.
[39] R. Hill, Proc. Phys. Soc. London 65 (1952) 350.
[40] S.F. Pugh, Philos. Mag. 45 (1954) 823.
[41] D. Koller, F. Tran, P. Blaha, 83 (2011) 195134; 85 (2012) 155109.
[42] H. Dixit, R. Saniz, S. Cottenier, D. Lamoen, B. Partoens, J. Phys. Condens. Matter 24 (2012) 205503.
[43] J.A. Camargo-Martinez, R. Baquero, Phys. Rev. B 86 (2012) 195106.
[44] N.V. Smith, Phys. Rev. B 3 (1971) 1862.
[45] H. Ehrenreich, M.H. Cohen, Phys. Rev. 115 (1959) 786.
[46] K. Ramesh Babu, Ch. Bheema Lingam, S. Auluck, Surya, P. Tewari, G. Vaitheeswaran, J. Solid State Chem. 184 (2011) 343.